Nonlocal solitons in the parametrically driven nonlinear Schrödinger equation: Stability analysis

Maxim A. Molchan*

Department of Mathematics and Applied Mathematics, University of Cape Town, Private Bag Rondebosch 7701, South Africa

(Received 28 September 2011; published 7 November 2011)

We study analytically and numerically the linear stability of weakly nonlocal solitons in the parametrically driven nonlinear Schrödinger equation. Two exact solutions are derived in an implicit form. We show analytically that despite the well-known stabilizing properties of nonlocality one of the solitons remains unstable even in the nonlocal case for any values of the dissipation, the damping, and the degree of nonlocality. The second soliton, as compared to its local counterpart, attains wider stable regions in the space of the parameters of the system.

DOI: 10.1103/PhysRevE.84.056603 PACS number(s): 05.45.Yv

I. INTRODUCTION

The parametrically driven, damped nonlinear Schrödinger equation (PDNLS)

$$i\psi_t + \psi_{xx} + 2\psi|\psi|^2 - \psi = h\psi^* - i\gamma\psi, \quad h,\gamma > 0, \tag{1.1}$$

describes a large number of nonlinear resonant phenomena in different media. This includes the Faraday resonance in fluid dynamics [1–3], parametric generation of spin waves in ferro and antiferromagnets [4,5], instabilities in plasma [6,7], amplitude generation in Josephson junctions [8,9], and signal amplification effects in fiber optics [10,11].

Solitary waves of Eq. (1.1) have been extensively studied in Refs. [5,12]. It was shown that Eq. (1.1) has two stationary soliton solutions, one of which is unstable for all values of the driver's strength h and the dissipation coefficient γ. The other solution is stable (for fixed γ) for small values of h and becomes unstable when h exceeds some threshold value. In Ref. [12] it was shown that depending on the values of h and γ three main scenarios in soliton dynamics can occur: the decay of the soliton to zero, single-mode chaotic oscillations of the amplitude and width, and the spatiotemporal chaos. The crucial role of radiation on the soliton's transformation within these regimes was studied in Ref. [13].

In the current paper we extend the model Eq. (1.1) to the nonlocal case,

$$i\psi_t + \psi_{xx} + 2\psi\int_{-\infty}^{+\infty} d\xi\, R(x-\xi)|\psi|^2(\xi) - \psi = h\psi^* - i\gamma\psi. \tag{1.2}$$

Here $R(x)$ is a symmetric response function of the nonlocal nonlinear medium [14,15]. We consider this equation in the limit of weak nonlocality when the size of the distribution of $|\psi(x)|^2$ in Eq. (1.2) in the transverse direction x is much larger than the spatial width of $R(x)$ [16]. Then expanding $\psi(\xi)$ in the vicinity of x leads to the PDNLS with an additional local term,

$$i\psi_t + \psi_{xx} + 2\psi|\psi|^2 + 2\varkappa\psi(|\psi|^2)_{xx} - \psi = h\psi^* - i\gamma\psi, \tag{1.3}$$

where $\varkappa = \frac{1}{2}\int_{-\infty}^{+\infty} dx x^2 R(x)$ is a small nonlocality parameter.

Nonlocality is typically a result of underlying transport processes such as heat conduction in thermal nonlinear media [17], diffusion of atoms in gases [18], long-range electrostatic interaction in liquid crystals [19], charge carrier transfer in photorefractive crystals [20], and many-body interaction in Bose-Einstein condensates [21]. It has proven to have a great impact on basic properties such as stabilization and propagation dynamics of localized structures. As shown in the earlier theoretical studies of the basic properties of such systems [22,23] this is due to the fact that nonlocality dramatically affects the formation and interaction of solitons.

In the current paper we examine the linear stability of two weakly nonlocal solitons of Eq. (1.3) with respect to *arbitrary square integrable perturbations* both analytically and numerically. We rigorously show that despite the notorious stabilizing property of nonlocality one of the solitons remains unstable even in the nonlocal case for any choice of the parameters $\varkappa$, h, and γ. At the same time, the second nonlocal soliton is stabilized considerably in the parameter space (h, γ) having wider regions of stability than its local counterpart.

The paper is organized as follows. In Sec. II we derive two exact solutions of Eq. (1.3) and perform the linearization about these solutions. In Sec. III we utilize the maximum principle to prove that one of the solutions is always unstable for all values of h, γ, and $\varkappa$. In Sec. IV we construct the perturbation theory for the second solution and demonstrate analytically its stability in the vicinity of the bifurcation line $h = \gamma$. In Sec. V we numerically investigate the stability properties of the second solution for arbitrary h, γ, and $\varkappa$ and provide the corresponding stability diagram. Finally, the results are summarized in Sec. VI.

II. EXACT SOLUTIONS AND THE LINEARIZED SYSTEM

Equation (1.3) has two stationary solitary wave solutions of the form

$$\psi^{\pm}(x) = \phi^{\pm}e^{-i\theta_{\pm}}, \tag{2.1}$$

where

$$\theta_+ = \frac{1}{2}\arcsin\left(\frac{\gamma}{h}\right), \quad \theta_- = \frac{\pi}{2} - \theta_+,$$

*m.moltschan@gmail.com

and the real-valued functions $\phi^{\pm}$ satisfy the equations

$$(1+4\varkappa\phi^2)\phi'' + 4\varkappa\phi(\phi')^2 - A_{\pm}^2\phi + 2\phi^3 = 0, \quad (2.2)$$

$$A_{\pm}^2 = 1 \pm \sqrt{h^2-\gamma^2}, \quad (2.3)$$

where the prime denotes the differentiation with respect to x. In Eqs. (2.2) ϕ stands for ϕ^+ or ϕ^- depending whether we take A_+ or A_-. Integrating Eqs. (2.2) twice gives the implicit expressions for $\phi = \phi^{\pm}$,

$$F(\phi,x) = 0,$$

$$F = A\sqrt{\varkappa}\arctan\left\{\frac{1+8\varkappa\phi-4A_{\pm}^2\varkappa}{4\sqrt{[\varkappa(A_{\pm}^2-\phi^2)(1+\varkappa\phi^2)]}}\right\} + \ln\left(\frac{\sqrt{A_{\pm}}\phi}{\sqrt{A_{\pm}^2-\phi^2+A_{\pm}\sqrt{1+\varkappa\phi^2}}}\right) + A_{\pm}(|x|-C_{\pm}), \quad (2.4)$$

where the constants of integration $C_{\pm} = \frac{\sqrt{\varkappa}\pi}{2} + A_{\pm}^{-1}\ln[A_{\pm}^{-1}(1+4\varkappa A_{\pm}^2)]$ are chosen to center the solutions at the origin. Solitary waves Eq. (2.1) may arise in resonant experiments on quasi-one-dimensional exchange-dipole spin-waves propagation in thin ferromagnetic films [24].

Equation (2.3) carries the information on the domain of existence of the two solutions on the (h,γ) parameter plane. The ψ^+ solution exists for any $h>0$ and, consequently, $A_+^2 > 1$. The existence domain of the solution ψ_- is bounded: $\gamma < h < \sqrt{1+\gamma^2}$ and $0 < A_-^2 < 1$. On the bifurcation line $h=\gamma$ $(A_+^2 = A_-^2 = 1)$ both solutions coincide. In Fig. 1 we present the profiles of the weakly nonlocal solitary waves Eq. (2.1) for $A_+^2 = A_+^2 = 1$ and different values of the nonlocality parameter $\varkappa$. As seen, nonlocality enhances the widths of the solutions without changing the maximum value of the humps at the origin.

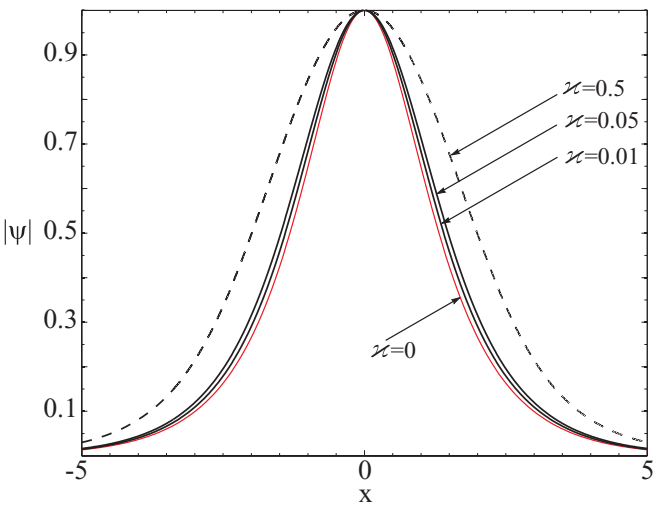

FIG. 1. (Color online) Spatial profiles of the solitary wave solutions Eq. (2.1) for different values of the nonlocality parameter $\varkappa$: dashed curve corresponds to $\varkappa = 0.5$; solid curves: the local case $\varkappa = 0$ (bottom), $\varkappa = 0.01$ (middle), and $\varkappa = 0.05$ (top).

It is also worthwhile to derive the explicit expansions of the profiles $\phi^{\pm}$ over the nonlocality parameter $\varkappa$:

$$\phi^{\pm} = f_0^{\pm} + \varkappa f_1^{\pm} + \varkappa^2 f_2^{\pm} + \cdots, \quad (2.5)$$

where

$$f_0^{\pm} = A_{\pm}\mathrm{sech}X,$$
$$f_1^{\pm} = A_{\pm}^3\mathrm{sech}X\tanh^2 X,$$
$$f_2^{\pm} = \frac{A_{\pm}^5}{3}(\cosh 2X - 25)\,\mathrm{sech}^3 X\tanh^2 X,$$
$$X \equiv A_{\pm}x.$$

In the limit $\varkappa \to 0$ Eqs. (2.4) and (2.5) reproduce the local solution of Ref. [5]: $\psi^{\pm} = A_{\pm}\mathrm{sech}\,(A_{\pm}x)\,e^{-i\theta_{\pm}}$.

To analyze the linear stability of the solutions Eq. (2.1) we write $\psi(x,t) = \psi^{\pm} + \delta\psi(x,t)$ and linearize in $\delta\psi$. Letting

$$\delta\psi(x,t) = e^{-\gamma t}\,[u(x,t) + iv(x,t)]\,e^{-i\theta_{\pm}} \quad (2.6)$$

yields

$$u_t - \gamma u = \mathcal{L}_0 v, \quad -v_t - \gamma v = \mathcal{L}_1 u, \quad (2.7)$$

where

$$\mathcal{L}_0 = -\frac{d^2}{dx^2} + 2 - A_{\pm}^2 - 2\phi^2 - 2\varkappa(\phi^2)'', \quad (2.8)$$

$$\mathcal{L}_1 = \mathcal{L}_1^{(0)} + \varkappa\mathcal{L}_1^{(1)}, \quad (2.9)$$

and

$$\mathcal{L}_1^{(0)} = -\frac{d^2}{dx^2} + A_{\pm}^2 - 6\phi^2, \quad (2.10)$$

$$\mathcal{L}_1^{(1)} = -\frac{d}{dx}\left(4\phi^2\frac{d}{dx}\right) - 2(\phi^2)'' - 4\phi\phi''. \quad (2.11)$$

In Eqs. (2.8)–(2.11) ϕ again stands for ϕ^+ or ϕ^-.

We impose the general restrictions on the perturbations u and v in Eqs. (2.7): They are represented by square integrable functions on the whole line $-\infty < x < \infty$. The solution is deemed unstable provided Eqs. (2.7) have solutions growing faster than $\exp(\gamma t)$ in time. Aiming to elucidate the general influence of the additional term in Eq. (1.3) stemming from the nonlocality of the initial equation (1.2), we shall not also restrict $\varkappa$ by very small values (we take $0 \leqslant \varkappa \leqslant 0.5$).

III. INSTABILITY OF ψ^-

The ψ^-–solution is amenable to the analytical treatment. First, we note that the operator $\mathcal{L}_0$ [Eq. (2.8)] can be presented in the following form:

$$\mathcal{L}_0 u = -\phi^{-1}\frac{d}{dx}\left[\phi^2\frac{d}{dx}(\phi^{-1}u)\right] + 2(1-A_-^2)u, \quad (3.1)$$

where $\phi = \phi^-$. Introducing the notation

$$\langle f\,|\,g\rangle = \int_{-\infty}^{\infty} f(x)g(x)\,dx$$

for the norm of $\mathcal{L}_0$ we immediately get

$$\langle u|\mathcal{L}_0 u\rangle = \int_{-\infty}^{\infty}\left[\phi\frac{d}{dx}(\phi^{-1}u)\right]^2 dx + 2(1-A_-^2)\int_{-\infty}^{\infty}u^2\,dx > 0. \tag{3.2}$$

Thus, the operator $\mathcal{L}_0$ is positive definite and invertible for all square integrable perturbations u. Equations (2.7) can now be rewritten as

$$\mathcal{L}_0^{-1}u_{tt} = \left(\gamma^2\mathcal{L}_0^{-1} - \mathcal{L}_1\right)u. \tag{3.3}$$

According to the maximum principle of Refs. [25,26], the maximum exponential growth rate Γ of solutions of Eq. (3.3) is given by

$$\Gamma^2 = \sup_u \frac{\langle u|\gamma^2\mathcal{L}_0^{-1} - \mathcal{L}_1|u\rangle}{\langle u|\mathcal{L}_0^{-1}|u\rangle} = \gamma^2 + \sup_u \frac{\langle u| - \mathcal{L}_1|u\rangle}{\langle u|\mathcal{L}_0^{-1}|u\rangle}. \tag{3.4}$$

If the quadratic form $\langle u| - \mathcal{L}_1|u\rangle$ in Eq. (3.3) attains positive values on some functions u, then the solitary wave is unstable. To demonstrate this, we rewrite the quadratic form of the operator $\mathcal{L}_1$ as follows:

$$\langle u|\mathcal{L}_1 u\rangle = \langle u|\mathcal{L}_0 u\rangle - 2(1-A_-^2)\langle u|u\rangle - 4\langle u|\phi^2 u\rangle + \varkappa\langle u|\mathcal{L}_1^{(1)}u\rangle. \tag{3.5}$$

As follows from Eq. (3.2), the first term in Eq. (3.5) attains the minimum zero value for $A_-^2 = 1$ and $u = \phi^-$. At the same time, the operator $\mathcal{L}_1^{(1)}$ is bounded, $\langle u|\mathcal{L}_1^{(1)}u\rangle < \infty$, then for sufficiently small $\varkappa$ the whole norm $\langle u|\mathcal{L}_1 u\rangle$ inevitably takes negative values. For example, using Eq. (2.5) and taking the perturbation in the form of the local solution $u_0 = A_-\mathrm{sech}(A_- x)$ gives

$$\langle u_0|\mathcal{L}_1 u_0\rangle = -\frac{16A_-^3}{3} + \frac{32A_-^5}{15}\varkappa + \cdots < 0.$$

That is, the weakly nonlocal solitary wave ψ_- is unstable with respect to its local counterpart.

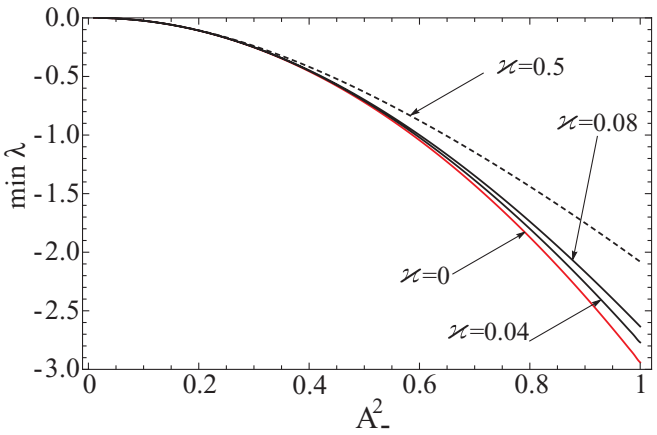

FIG. 2. (Color online) The minimum discrete eigenvalue of the operator $\mathcal{L}_1$ as a function of the amplitude A_-^2. Here the dashed curve corresponds to $\varkappa = 0.5$; the bottom, middle, and top solid curves correspond to $\varkappa = 0$, $\varkappa = 0.04$, and $\varkappa = 0.08$, respectively.

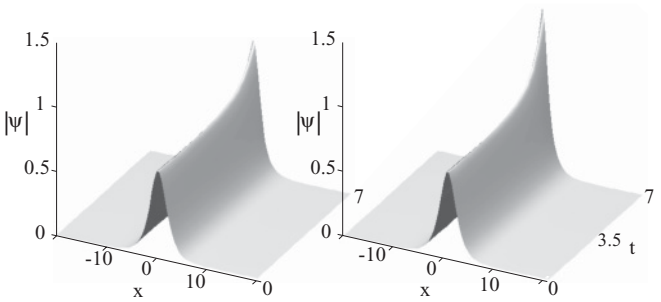

FIG. 3. Development of instability for the local ψ^-–solution $\varkappa = 0$ (right) and weakly nonlocal $\varkappa = 0.05$ (left). Here $h = 0.5$ and $\gamma = 0.2$.

In Fig. 2 we present the minimum discrete eigenvalue λ of the operator $\mathcal{L}_1$ as a function of the amplitude A_-^2 (the dashed curve corresponds to $\varkappa = 0.5$; the bottom, middle, and top solid curves correspond to $\varkappa = 0$, $\varkappa = 0.04$, and $\varkappa = 0.08$, respectively). Obviously the operator $\mathcal{L}_1$ has negative eigenvalues for all A_-^2 and $\varkappa$. Consequently, the ψ^-–solution is unstable with respect to arbitrary square integrable perturbations for any choice of h, γ, and $\varkappa$.

As follows from Fig. 2, the nonlocality reduces the unstable growth rates and tends to suppress the development of instability. In Fig. 3 we present the development of instability for local (right) and nonlocal (left, $\varkappa = 0.08$) solitary solutions obtained by the direct numerical integration of Eq. (1.3). The nonlocal solution demonstrates the lower growth rate of instability as compared to the local one, though the solution remains unstable in general.

IV. STABILITY OF ψ^+ NEAR THE BIFURCATION LINE $h = \gamma$

In this section we consider the stability properties of the ψ^+–solution when the driver's strength h is close to the dissipation parameter γ, $h \sim \gamma$. We introduce the small parameter $\varepsilon \ll 1$ defined via the expression

$$A_+^2 = 1 + \sqrt{h^2 - \gamma^2} = 1 + \varepsilon$$

and impose the following ansatz for the perturbations u and v in Eqs. (2.7):

$$u(x,t) = U(x)e^{(\Lambda+\gamma)t}, \quad v(x,t) = V(x)e^{(\Lambda+\gamma)t}, \tag{4.1}$$

where Λ is real. Obviously, the solution is stable (unstable) provided $\Lambda < 0$ ($\Lambda > 0$). Now, the eigenvalue problem Eqs. (2.7) can be presented in the following matrix form:

$$\mathcal{L}\begin{pmatrix} U \\ V \end{pmatrix} = \Lambda\begin{pmatrix} U \\ V \end{pmatrix}, \tag{4.2}$$

where

$$\mathcal{L} = \begin{pmatrix} 0 & \mathcal{L}_0 \\ -\mathcal{L}_1 & -2\gamma \end{pmatrix}. \tag{4.3}$$

When $h = \gamma$ the spectrum of the eigenvalue problem Eq. (4.2) coincides with that for an undamped undriven weakly nonlocal NLS soliton. The spectrum fills the imaginary axis with a gap separated by the zero. As h deviates from γ the phase invariance is broken and the split of the zero eigenvalue occurs (Fig. 4). These emerging eigenvalues may lead to the

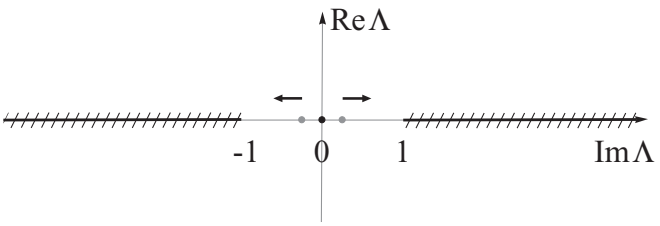

FIG. 4. Split of the zero eigenvalue of the operator $\mathcal{L}$ for $h \neq \gamma$.

instability of the solution. We now evaluate the positions of these eigenvalues.

Combining two equations in Eq. (4.2) we get

$$\mathcal{L}_1 \mathcal{L}_0 V = \lambda V, \tag{4.4}$$

where

$$\lambda = -\Lambda\,(\Lambda + 2\gamma)\,. \tag{4.5}$$

Proceeding to the perturbation analysis we write the following expansions:

$$\begin{aligned} \lambda &= \lambda_0 + \varepsilon\lambda_1 + \cdots, \\ V &= V_0 + \varepsilon V_1 + \cdots, \\ \mathcal{L}_{0,1} &= \mathcal{L}^0_{0,1} + \varepsilon\mathcal{L}^1_{0,1} + \cdots. \end{aligned} \tag{4.6}$$

We consider the split of the zero eigenvalue, then $\lambda_0 = 0$ and at the order $O(\varepsilon^0)$ the equation yields $\mathcal{L}^0_0 V_0 = 0$ with $V_0 = \phi_0$, where we have introduced the notation $\phi_0 = \phi^+|_{h=\gamma}$.

At the first order we get

$$\mathcal{L}^0_1\mathcal{L}^1_0\phi_0 + \mathcal{L}^0_1\mathcal{L}^0_0 V_1 = \lambda_1\phi_0. \tag{4.7}$$

Multiplying both sides of Eq. (4.7) by $\phi_0(\mathcal{L}^0_1)^{-1}$ and integrating over the whole line $-\infty < x < \infty$ for the eigenvalue λ_1 we get

$$\lambda_1 = \frac{\langle \mathcal{L}^1_0\phi_0|\phi_0\rangle}{\langle (\mathcal{L}^0_1)^{-1}\phi_0|\phi_0\rangle}. \tag{4.8}$$

In deriving Eq. (4.8) we took into account that $\langle\phi_0|\mathcal{L}^0_0 V_1\rangle = \langle\mathcal{L}^0_0\phi_0|V_1\rangle = 0$.

To calculate the denominator in Eq. (4.8) we solve the equation

$$\left(\mathcal{L}^0_1\right)^{-1}\phi_0 = \Phi_0$$

or

$$\mathcal{L}^0_1\Phi_0 = \phi_0.$$

The function Φ_0 can be found using the standard procedure of the variation of parameters:

$$\Phi_0 = \mathrm{Re}\left\{-\frac{\phi_0}{2} - \frac{\phi_0}{i - 2\sqrt{\varkappa}}\sqrt{\frac{1-\phi_0^2}{1+4\varkappa\phi_0^2}} \times \left[F(\Psi|\kappa^2) - 2\Pi(\kappa,\Psi|\kappa^2)\right]\right\}, \tag{4.9}$$

where F and Π are the complete and incomplete elliptic integrals of the first and third types, respectively, $\Psi = \arcsin(\sqrt{(1+\phi_0)/(1-\phi_0)}/\sqrt{k})$ and $k = (2\sqrt{\varkappa}+i)/(2\sqrt{\varkappa}-i)$. In Fig. 5 we provide the plots of Φ_0 for different values of $\varkappa$.

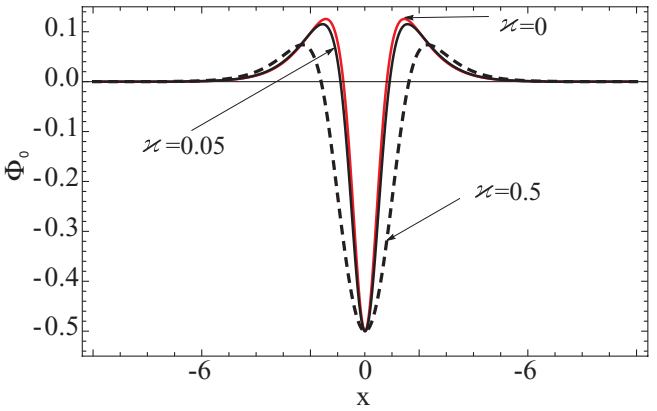

FIG. 5. (Color online) Plots of the function Φ_0 [Eq. (4.9)] for different values of the parameters $\varkappa$: $\varkappa = 0.5$ (dashed curve), $\varkappa = 0$ (solid top curve), and $\varkappa = 0.05$ (solid bottom curve).

Finally, the eigenvalue λ_1 to the first order of approximation is given by the expression

$$\lambda_1 = \frac{\langle \mathcal{L}^1_0\phi_0|\phi_0\rangle}{\langle \Phi_0|\phi_0\rangle}, \tag{4.10}$$

where

$$\begin{aligned} \mathcal{L}^1_0 &= -1 - \frac{4\phi_0(1+4\varkappa)}{(1+4\varkappa\phi_0^2)^3}\frac{\partial\phi_0}{\partial\epsilon}\bigg|_{\epsilon=0}, \quad \frac{\partial\phi_0}{\partial\epsilon}\bigg|_{\epsilon=0} \\ &= \frac{\phi_0}{2}\left[1 - \frac{\sqrt{1-\phi_0^2}}{1+4\varkappa\phi_0^2}\ln\left(\frac{\sqrt{1-\phi_0^2}+\sqrt{1+4\varkappa\phi_0^2}}{\phi_0\sqrt{1+4\varkappa}}\right)\right]. \end{aligned} \tag{4.11}$$

As follows from Eqs. (4.9) and (4.11), the functions Φ_0 and $\mathcal{L}^1_0$ do not contain the variable x explicitly. Then the integrals in Eq. (4.10) can be calculated without restoring the dependence of ϕ_0 on x from Eq. (2.4). This is achieved by the change of the integration variable:

$$\int_{-\infty}^{\infty} f\,[\phi_0(x)]\,dx = 2\int_0^1 \frac{f(y)}{y'}\,dy,$$

where $y' = y\sqrt{(1-y^2)/(1+4\varkappa y^2)}$ and $f(x)$ is an arbitrary even function of the variable x [note that $\mathcal{L}^1_0$ and Φ_0 in Eq. (4.10) are even functions of x].

From Eq. (4.5) the maximum eigenvalue of the operator $\mathcal{L}$ yields

$$\Lambda = -\gamma + \sqrt{\gamma^2 - \varepsilon\lambda_1}. \tag{4.12}$$

If λ_1 is positive (negative) then $\Lambda < 0\,(\Lambda > 0)$ and the solitary wave is stable (unstable). In Fig. 6 we present the dependence of λ_1 on the nonlocality parameter $\varkappa$. Obviously, λ_1 is positive for all $\varkappa$. Consequently, the ψ^+–solution is stable for all $\varkappa$ and $h \sim \gamma$.

As follows from Eqs. (2.6) and (4.1), the rate of the decay of the perturbation v is given by $\Gamma = |\Lambda|$. Increasing the degree of nonlocality $\varkappa$, we decrease λ_1 and, consequently, Γ. Thus, nonlocality suppresses both the growth rate of instability in the case of unstable perturbations and the rate of the decay of the perturbation in stable contexts.

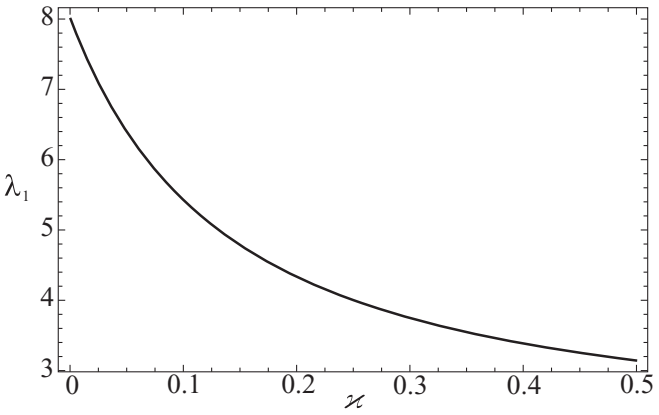

FIG. 6. The splitting eigenvalue λ_1 as a function of the nonlocality parameter $\varkappa$.

V. STABILITY DIAGRAM FOR ψ^+–SOLUTION

To determine stability properties of the ψ^+–solution for arbitrary values of h and γ we solved the eigenvalue problem Eq. (4.2) numerically within the intervals $0 < h,\gamma < 1.5$. The results are presented in Fig. 7. The solitary wave ψ^+ exists above the line $h = \gamma$ and is unstable with respect to continuous spectrum excitations for $h > \sqrt{1+\gamma^2}$ (see, e.g., Ref. [5]). The stability properties of ψ^+ with respect to local mode perturbations crucially depend on the value of the nonlocality parameter $\varkappa$. The local soliton ($\varkappa = 0$) is stable in the region A in Fig. 7. Increasing the nonlocality degree results in the increased stability domains. The weakly nonlocal solution with $\varkappa = 0.05$ is stable in A and attains an additional stability region B, while for $\varkappa = 0.5$ the solitary wave is stable in the regions A, B, and C. Obviously, nonlocality favors the suppression of instability for the ψ^+–solution.

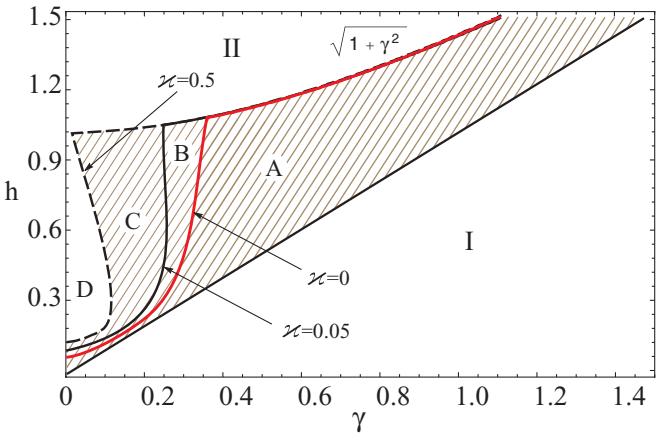

FIG. 7. (Color online) Stability diagram for the ψ^+–solution. In the domain I ($h < \gamma$) no nontrivial solutions exist. In the domain II ($h > \sqrt{1+\gamma^2}$) the solution ψ^+ exists but is unstable with respect to continuous spectrum perturbations. Dashed domains correspond to the regions of linear stability of the ψ^+ solitary wave: $\varkappa = 0$ (A), $\varkappa = 0.05$ (A and B), and $\varkappa = 0.5$ (A, B, and C). The solution is unstable with respect to local mode perturbations in D for $\varkappa = 0.5$, D and C for $\varkappa = 0.05$, and D, C, and B for the local soliton $\varkappa = 0$.

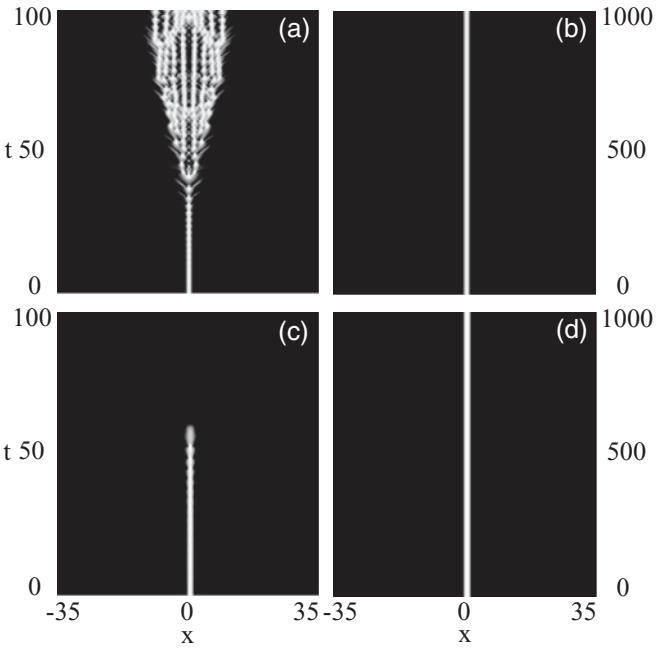

FIG. 8. Evolution of the local [$\varkappa = 0$, (a) and (c)] and nonlocal [$\varkappa = 0.05$, (b) and (d)] ψ^+–solution for different sets of the parameters h and γ: $h = 1.1$ and $\gamma = 0.3$ in (a) and (b); $h = 0.7$ and $\gamma = 0.3$ in (c) and (d). On all plots the contour plots of $|\psi^+|$ are depicted.

We confirmed the predictions of linear stability analysis by the direct numerical integration of Eq. (1.3), taking the perturbation Eq. (2.6) in the form $\delta\psi(x,t=0) = 10^{-4}\mathrm{sech}(x)e^{-i\theta_+}$. In Fig. 8 we provide the evolution of the ψ^+ solution (contour plots of $|\psi^+|$ are depicted) for two different sets of the parameters h and γ: $h = 1.1$ and $\gamma = 0.3$ for Figs. 8(a) and 8(b) and $h = 0.7$ and $\gamma = 0.3$ for Figs. 8(c) and 8(d). In Fig. 8(a) the local soliton ($\varkappa = 0$) undergoes the transition to the spatiotemporal chaos, while in Fig. 8(c) the solution decays to zero. In Figs. 8(b) and 8(d) the corresponding evolution of the nonlocal ($\varkappa = 0.05$) solitary wave is presented. In both cases the nonlocal solution is stable.

VI. CONCLUSIONS

In this paper we have studied analytically and numerically the linear stability of weakly nonlocal solitary waves of the parametrically driven, damped nonlinear equation. We considered the most general class of perturbations represented by square integrable functions.

Though the solutions can be derived in an implicit form only, we establish two analytical facts. First, using the maximum principle we prove that one of the solitary wave solutions remains unstable in the nonlocal case, despite the well-known stabilizing effect of nonlocality. Second, we show that the second solution is stable in the vicinity of the bifurcation line $h = \gamma$ (that is, when the value of the driver's strength is close enough to the value of the dissipation parameter γ). We also perform the numerical investigation of the corresponding eigenvalue problem and obtain the stability diagram for the second solitary wave. The nonlocality is shown to extend the domains of linear stability in the (h, γ)-plane. The results of

the direct numerical integration of the governing equation are in perfect agreement with the predictions of the linear stability analysis.

ACKNOWLEDGMENT

The author was supported by the National Research Foundation (NRF) of South Africa.

[1] C. Elphick and E. Meron, Phys. Rev. A **40**, 3226 (1989).
[2] J. R. Yan and R. J. Mei, Europhys. Lett. **23**, 335 (1993).
[3] X. Wang and R. Wei, Phys. Rev. Lett. **78**, 2744 (1997).
[4] H. Yamazaki and M. Mino, Prog. Theor. Phys. Suppl. **98**, 400 (1989).
[5] I. V. Barashenkov, M. M. Bogdan, and V. I. Korobov, Europhys. Lett. **15**, 113 (1991).
[6] V. E. Zakharov, S. L. Musher, and A. M. Rubenchik, Phys. Rep. **129**, 285 (1985).
[7] N. Yajima and M. Tanaka, Prog. Theor. Phys. Suppl. **94**, 138 (1988).
[8] C. Vanneste, A. Gilabert, P. Sibillot, and D. B. Ostrowsky, J. Low Temp. Phys. **45**, 517 (1981).
[9] G. Cicogna and L. Fronzoni, Phys. Rev. A **42**, 1901 (1990).
[10] I. H. Deutsch and I. Abram, J. Opt. Soc. Am. B **11**, 2303 (1994).
[11] A. Mecozzi, L. Kath, P. Kumar, and C. G. Goedde, Opt. Lett. **19**, 2050 (1994).
[12] M. Bondila, I. V. Barashenkov, and M. M. Bogdan, Physica D **87**, 314 (1995).
[13] V. S. Shchesnovich and I. V. Barashenkov, Physica D **164**, 83 (2002).
[14] W. Krolikowski, O. Bang, J. J. Rasmussen, and J. Wyller, Phys. Rev. E **64**, 016612 (2001).
[15] E. V. Doktorov and M. A. Molchan, Phys. Rev. A **75**, 053819 (2007).
[16] W. Krolikowski and O. Bang, Phys. Rev. E **63**, 016610 (2000).
[17] A. Dreischuh, G. G. Paulus, F. Zacher, F. Grasbon, and H. Walther, Phys. Rev. E **60**, 6111 (1999).
[18] D. Suter and T. Blasberg, Phys. Rev. A **48**, 4583 (1993).
[19] C. Conti, M. Peccianti, and G. Assanto, Phys. Rev. Lett. **92**, 113902 (2004).
[20] M. Segev, B. Crosignani, A. Yariv, and B. Fischer, Phys. Rev. Lett. **68**, 923 (1992).
[21] V. M. Perez-Garcia, V. V. Konotop, and J. J. Garcia-Ripoll, Phys. Rev. E **62**, 4300 (2000).
[22] A. Dreischuh, D. Neshev, D. E. Petersen, O. Bang, and W. Krolikowski, Phys. Rev. Lett. **96**, 043901 (2006).
[23] O. Bang, W. Krolikowski, J. Wyller, and J. J. Rasmussen, Phys. Rev. E **66**, 046619 (2002).
[24] V. V. Kiselev and A. P. Tankeyev, J. Phys. Condens. Matter **8**, 10219 (1996).
[25] G. Laval, C. Mercier, and R. Pellat, Nucl. Fusion **5**, 156 (1965).
[26] E. W. Laedke and K. H. Spatschek, Physica D **5**, 227 (1982).